The Crystal Structure of the *Escherichia coli* Maltodextrin Phosphorylase−Acarbose Complex[†,‡]

M. O'Reilly,[§] K. A. Watson, and L. N. Johnson*

Laboratory of Molecular Biophysics and Oxford Centre for Molecular Sciences, Department of Biochemistry, University of Oxford, Rex Richards Building, South Parks Road, Oxford OX1 3QU, U.K.

Received December 3, 1998; Revised Manuscript Received January 29, 1999

ABSTRACT: Acarbose is a naturally occurring pseudo-tetrasaccharide. It has been used in conjunction with other drugs in the treatment of diabetes where it acts as an inhibitor of intestinal glucosidases. To probe the interactions of acarbose with other carbohydrate recognition enzymes, the crystal structure of *E. coli* maltodextrin phosphorylase (MalP) complexed with acarbose has been determined at 2.95 Å resolution and refined to crystallographic *R*-values of *R* (R_{free}) = 0.241 (0.293), respectively. Acarbose adopts a conformation that is close to its major minimum free energy conformation in the MalP−acarbose structure. The acarviosine moiety of acarbose occupies sub-sites +1 and +2 and the disaccharide sub-sites +3 and +4. (The site of phosphorolysis is between sub-sites −1 and +1.) This is the first identification of sub-sites +3 and +4 of MalP. Interactions of the glucosyl residues in sub-sites +2 and +4 are dominated by carbohydrate stacking interactions with tyrosine residues. These tyrosines (Tyr280 and Tyr613, respectively, in the rabbit muscle phosphorylase numbering scheme) are conserved in all species of phosphorylase. A glycerol molecule from the cryoprotectant occupies sub-site −1. The identification of four oligosaccharide sub-sites, that extend from the interior of the phosphorylase close to the catalytic site to the exterior surface of MalP, provides a structural rationalization of the substrate selectivity of MalP for a pentasaccharide substrate. Crystallographic binding studies of acarbose with amylases, glucoamylases, and glycosyltranferases and NMR studies of acarbose in solution have shown that acarbose can adopt two different conformations. This flexibility allows acarbose to target a number of different enzymes. The two alternative conformations of acarbose when bound to different carbohydrate enzymes are discussed.

Naturally occurring α-glucan hydrolase inhibitors have been identified in animal, plant, fungal, and bacterial systems and are of interest for the development of treatments of diabetes and other carbohydrate metabolism diseases. Acarbose is a member of the trestatin family of pseudo-oligosaccharides that act as potent inhibitors of α-amylases, glucoamylases, α-glucosidases, and cyclodextrin glucosyltransferase (CGTases)[1] (K_i in the range of 10^{-5}−10^{-10} M) (*1*). Acarbose has been used by itself and with other agents in the treatment of non-insulin-dependent diabetes (*2*, *3*). It has proved effective in contributing to glycemic control by delaying carbohydrate digestion and subsequent absorption of glucose. Members of the acarbose family contain a structural template comprised of an acarviosine group [a cyclitol ring (hydroxymethylconduritol unit) linked to a 4-amino-4,6-dideoxy-D-glucopyranose via a α-1,4-linkage]. Acarbose is a pseudo-tetrasaccharide with two glucosyl groups attached to the reducing end of the acarviosine moiety (Figure 1). In the trestatins, varying numbers of α-(1,4)-D-glucopyranose rings may be attached to the reducing and/or nonreducing ends of the acarviosine template.

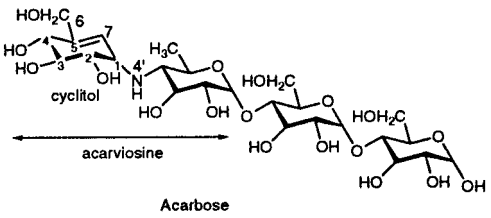

FIGURE 1: Acarbose. The acarviosine moiety composed of the cyclitol (hydroxymethylconduritol unit) and 4-amino-4,6-dideoxy-D-glucose is indicated.

In solution and in the crystalline state, α-(1,4)-linked glucosyl sugars adopt a minimum free energy conformation in which the 2-hydroxyl from one glucopyranose ring forms an intramolecular hydrogen bond with the 3-hydroxyl of the adjacent glucopyranose (*4*−*6*). In solution at neutral and alkali pH, the acarviosine moiety of acarbose also adopts this preferred conformation (*7*, *8*). At acid pH, a second minimum energy conformation is populated to a significant degree (*8*). This flexibility in conformation, representing different torsion angles about the aminoglycosidic bond, is exploited by different hydrolases in recognition of acarbose (Figure 2). The preferred minimum energy conformation is recognized by the *exo*-amylase, glucoamylase from *Aspergil-*

[†] This work has been supported by the MRC and the British Diabetic Association.

[‡] Coordinates have been deposited in the Brookhaven Protein Data Bank with accession number 2ECP.

* To whom correspondence should be addressed. Telephone: 44-1865-275365. Fax: 44-1865-510454. E-mail: Louise@biop.ox.ac.uk.

[§] Current address: MRC Laboratory of Molecular Biology, Hills Rd., Cambridge CB2 2QH, U.K.

[1] Abbreviations: MalP, *E. coli* maltodextrin phosphorylase; GP, rabbit muscle glycogen phosphorylase; CGTase, cyclodextrin glycosyltransferase.

10.1021/bi9828573 CCC: $18.00
Published on Web 04/09/1999

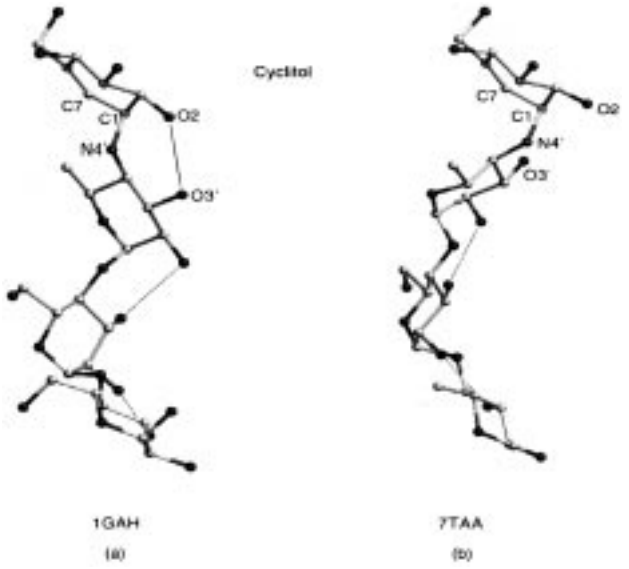

FIGURE 2: Two different conformations of acarbose observed bound to different glucosidases. (a) The major minimum energy conformation as observed in acarbose binding to glucoamylase (10) in which there is a hydrogen bond between the O2 hydroxyl of the cyclitol and the O3 hydroxyl of the 6-deoxy sugar. PDB coordinate 1GAH. $\phi = (C7-C1-N4'-C4') = 104.0°$, $\psi = (C1'-N4'-C4'-C5') = -112.8°$. (b) The secondary minimum energy conformation as observed in acarbose binding to TAKA amylase (15) in which there is no intramolecular hydrogen bond between the cyclitol and the 6-deoxy sugar. PDB coordinate 7TAA. $\phi = (C7-C1-N4'-C4') = 32.8°$, $\psi = (C1-N4'-C4'-C5') = -151.6°$.

lus awamori, an enzyme that hydrolyzes terminal α-(1,4)-D-glycosidic bonds from the nonreducing ends of maltooligosaccharides to produce *β*-D-glucose (*9*−*11*). The secondary minimum energy conformation of acarbose is recognized by the *endo*-amylases (*12*−*16*) and by cyclodextrin glycosyltransferase (CGTase) (*17*−*19*). These enzymes hydrolyze the α-(1,4)-D-glycosidic bond within an oligosaccharide, and the reaction proceeds with retention of configuration. The flexibility in conformation may contribute to the ability of acarbose to inhibit a number of different enzymes, but other factors are also important.

Early work had shown that the inhibitory properties of acarbose with respect to α-hydrolases are dependent upon the acarviosine group as a whole, and not the individual cyclitol or amino sugar units (*1*). The conformation of the cyclitol ring of acarbose is constrained by the double bond between C5 and C7 (corresponding to the endocyclic O5 of glucose). The double bond promotes an $^2H_3$ half-chair (*H*) conformation in which atoms C4, C5, C7, and C1 are coplanar and atoms C2 and C3 are above and below the plane, respectively. The cyclitol is often referred to as a transition state analogue of the oxonium/carbonium ion transition state anticipated for glycoside hydrolysis. However the $^2H_3$ conformation is not an ideal mimic either structurally or electronically of such a transition state. In the oxonium/carbonium ion intermediate, the partial double bond between the O5 and C1 atoms of the glucopyranose ring constrains the atoms C5, O5, C1, and C2 to be coplanar as in the $^4H_3$ half-chair or sofa conformation (*20*). Nevertheless, despite this lack of precise complementarity with the proposed transition state structure, comparative studies with glucoamylase on the binding of acarbose ($K_d = 9 \times 10^{-11}$ M) and the saturated D-glucodihydroacarbose ($K_d = 3 \times 10^{-7}$ M) have shown that the planar geometry of the cyclitol ring in acarbose does make a significant contribution to binding in this enzyme. In addition, a salt link between a carboxylate and the amino linkage between the cyclitol and the 6-deoxy sugar of acarbose is observed in all acarbose/carbohydrate enzyme structures to date (amylases, CGTase, and glucoamylase). This interaction appears to be an important factor explaining the high affinity of acarbose for these enzymes (*10*).

E. coli maltodextrin phosphorylase (MalP) (EC 2.4.1.1) is a 796 amino acid, nonallosteric, enzyme that is 46% identical in sequence to rabbit muscle glycogen phosphorylase (GP). Unlike GP, MalP is not regulated by phosphorylation or by allosteric effectors but is regulated by control of gene expression (*21*). Structural studies have provided an explanation for the lack of control properties in MalP at the protein level (*22*). The mammalian and bacterial phosphorylases exhibit nearly 100% identity in residues at the catalytic site, and both utilize the 5′-phosphate of the essential cofactor pyridoxal phosphate in catalysis. MalP catalyzes the phosphorolytic cleavage, from the nonreducing end, of α-1,4-linked maltodextrins $(Glc)_n$ to yield α-D-glucose-1-P (Glc-1-P):

$$(Glc)_n + P_i \leftrightarrow (Glc)_{n-1} + \text{Glc-1-P}$$

The enzyme prefers substrate maltodextrins with a minimum length of five glucosyl units for phosphorolysis and four glucosyl units for the reverse reaction of oligosaccharide synthesis (*23*).

MalP exhibits a higher affinity for oligosaccharide substrates than GP, and this observation has been exploited in order to detect binding of oligosaccharides at the catalytic site of phosphorylase. Following the terminology of Davies et al. (*24*), sub-sites for oligosaccharide recognition are numbered −1 to +4 from the nonreducing end to reducing end and the site of phosphorolysis (or hydrolysis in glucosidases) is between sub-sites −1 and +1. Co-crystallization studies with maltohexaose and MalP (*25*) showed a disaccharide, maltose, bound at sub-sites +1 and +2 at the catalytic site of MalP. These results identified a tyrosyl/carbohydrate interaction at sub-site +2. Mutagenesis studies showed that this tyrosine was of critical importance for substrate binding and recognition. Analysis of the oligosaccharide mixture from the co-crystallization experiments indicated that both catalysis and hydrolysis of the oligosaccharide had occurred over the period of crystallization. To address these problems with a nonhydrolyzable and nonphosphorylatable substrate, we have carried out binding studies with acarbose to *E. coli* MalP. The structural studies on the MalP−maltose complex had indicated that the conformation between the sugars in sub-sites −1 and +1 should be close to the secondary minimum energy conformation for acarbose (i.e., as in Figure 2b). It was anticipated that acarbose would bind in sub-sites −1 to +3 in this secondary conformation. The present studies show that acarbose binds at sub-sites +1 to +4 in its minimum free energy conformation (i.e., the conformation shown in Figure 2a). A further carbohydrate/aromatic interaction has been identified at sub-site +4. The weak binding is consistent with the poor inhibition constant observed for MalP inhibition by acarbose (K_i approximately 5 mM; R. Schinzel prelimi-

nary unpublished results) that suggests that acarbose is not a transition state analogue for the MalP-catalyzed reaction. The results contribute to an analysis of the recognition and conformation of acarbose by carbohydrate-recognizing enzymes and explain the substrate specificity of MalP.

EXPERIMENTAL PROCEDURES

Expression, Purification, and Crystallization. MalP was purified from *E. coli* ΔMalA518 cells harboring the expression plasmid pMAP101 as described previously *(26, 27)*. The purification steps involved ammonium sulfate precipitation, followed by Q-Sepharose anion exchange chromatography and a glycogen−glycine affinity column. Two additional purification steps were added. Protein solution at approximately 1.8 mg/mL in 20 mM Tris/HCl, pH 6.9, 1 mM EDTA was applied to a Pharmacia Superdex-200 gel filtration column. The pooled fractions in the above buffer were then passed over a Pharmacia Mono-Q anion exchange column and eluted with a 0−150 mM NaCl gradient. The pooled fractions were buffer-exchanged into 1 M Tris/HCl, pH 8.5.

Triangular block-like cocrystals of MalP with acarbose were grown over a 3 day period by the hanging-drop vapor diffusion method from drops containing 10 mg/mL MalP, 30 mM acarbose, 25−28% w/v PEG 3350, 0.1−0.6 M LiCl, and 0.1 M Tris/HCl, pH 8.5 at 18 °C.

Data Collection and Processing. Data were collected from a single crystal, space group $P2_12_12_1$, unit cell dimensions $a = 76.5$ Å, $b = 105.8$ Å, and $c = 217.7$ Å, and one dimer molecule of MalP per asymmetric unit. The crystal was soaked for <5 s in a cryoprotectant of 20% glycerol in the mother liquor and flash-frozen to 100 K. Data were collected on an 18 cm MAR Research image plate at the X-ray diffraction beamline in Elettra, Trieste, Italy. Exposures were 60 s for 1° and 0.5° oscillations, and a total of 92° of data were collected. The crystal to detector distance was 280 mm and X-ray wavelength 0.9 Å. The slits were set at 0.3 mm, and the ring current varied from 153 to 113 mA over the course of the data collection. The 18 cm MAR detector limited the resolution to 2.95 Å, although the crystals diffracted further.

Data were processed using MOSFLM 5.40 (Prerelease version from Dr. A. G. W. Leslie), that successfully integrated the closely spaced irregular shaped reflections, and data were scaled with SCALA. Intensities were reduced to structure factors with TRUNCATE (*28*).

Structure Determination. Co-crystallization of MalP with acarbose gave a new crystal form that was different from the native MalP and the oligosaccharide complex. The structure was solved by molecular replacement with AMORE (*29*) using a monomer subunit from the native MalP structure (*22*) as a search object placed in a 130 Å × 130 Å × 130 Å unit cell. Waters and noncovalently attached ligands were removed from the structure. Rotation solutions used a 30 Å search-radius and 6−4 Å resolution data. Translation solutions used 10−2.95 Å resolution data. The top solution to the rotation and translation functions gave a crystallographic $R = 44.3\%$ and a correlation coefficient of 43.7%. This solution was fixed and the position of the second subunit determined. The corresponding values of R and correlation coefficient were 34.3% and 69.1%, and these values improved to 32.0% and 74.8% after 50 cycles of rigid-body refinement with AMORE.

Table 1: Data Collection and Refinement Statistics for the *E. coli* MalP−Acarbose Complex

Data Collection	
resolution (highest range) Å	20−2.95 (3.11−2.95)
completeness (highest range) (%)	88.9 (78.2)
R_m[a] (highest range)	0.068 (0.157)
multiplicity	2.6
$\langle I/\sigma_I \rangle$	12.5
Refinement	
resolution range (Å)	15−2.95
no. of unique reflections (no. for R_f)	32524 (852)
final R (R_f)[b]	0.241 (0.293)
no. of atoms	
all	12961
acarbose	44
glycerol	6
waters	93
average B (Å^2)	
all	53.6
acarbose	60.0
glycerol	58.7
waters	49.1
rms deviation from ideal geometry	
bonds (Å)	0.009
angles (deg)	2.1
impropers (deg)	1.6
rms deviations in B-factors for covalently linked atoms (Å^2)	
all	2.7
main chain	2.0
side chain	3.3

[a] $R_m = \sum_h\sum_i|I(h) - I_i(h)|/\sum_h\sum_i I_i(h)$ where $I_i(h)$ and $I(h)$ are the ith and mean intensity values of reflection h-respectively. [b] Crystallographic $R = \sum_h|F_o - F_c|/\sum_h F_o$ where F_o and F_c are the observed and calculated structure factor amplitudes of reflection h, respectively. R_f, the free R factor, is calculated as for R, but using 2.5% of the data set that had been excluded from the refinement.

The structure was refined as a rigid body with X-PLOR (*30*), employing tight NCS constraints to give $R = 0.303$, $R_f = 0.309$. Initially data with $F > 2\sigma$ were used, but in the subsequent stages of the refinement, all data were included. After positional refinement, 2-fold NCS averaging, and solvent flattening, the $F_o - F_c$ and $2F_o - F_c$ electron density maps showed a glycerol molecule at sub-site −1 and the acarviosine moiety of the acarbose at sub-sites +1 and +2. These were included in the structure. Coordinates for the acarbose molecule were obtained from the coordinates of the acarbose-like molecule bound to porcine pancreatic amylase I (*12*) (Brookhaven Crystallographic Data Bank coordinate set 1PPI) that were in turn derived from those of Bock and Pedersen (*7*). Iterative cycles of refinement, using all data (15−2.95 Å) and tight NCS restraints, were continued using REFMAC (*31*). Difference density showed the additional two glucosyl units of acarbose at sub-sites +3 and +4, and these sugars were included. In amylases, the acarviosine unit of acarbose can be reshuffled by transglycosylation reactions. Such processing of the inhibitor can cause problems in interpretation of results. In this case, MalP is not able to catalyze transglycosylation, and so no reshuffling is expected. The presence of acarbose and the chain direction were confirmed by the lack of density for the O6 hydroxyl of sugar in the +2 site in both the A and B subunits and the presence of such density for each of the other glucosyl sites.

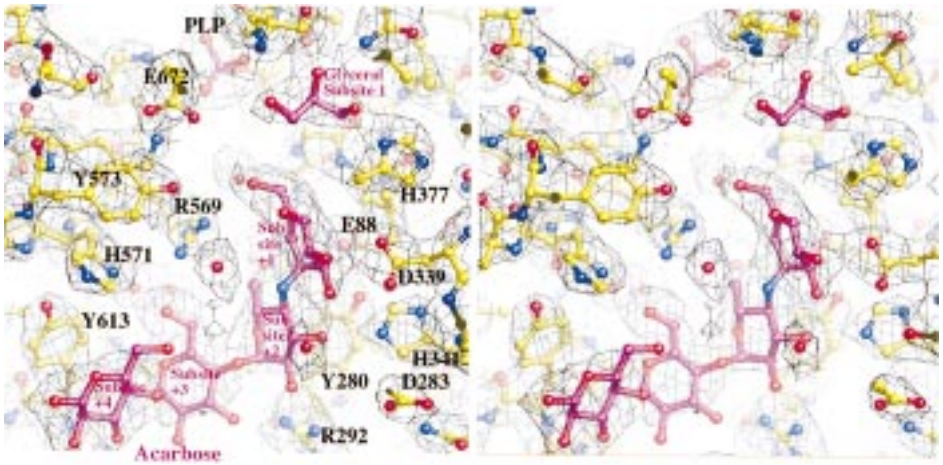

FIGURE 3: Stereodiagram of the electron density in the vicinity of the acarbose binding site in MalP (molecule A). The $2F_o - F_c$ electron density map calculated with the final coordinates from REFMAC is contoured at 0.85× the rms electron density. The final model coordinates are superimposed for the A molecule. This figure and Figures 4, 5, and 6 were produced by OGLOBJECTS (M. E. M. Noble, unpublished work).

Grouped, or individual, isotropic *B*-factor refinement within REFMAC produced similar refinement statistics. Thus, individual isotropic *B*-factor refinement was employed. An overall anisotropic temperature factor correction was applied to the original data using SCALEIT (*28*). A total of 93 waters were manually incorporated into the structure at sites exhibiting an $(F_o - F_c)$ peak $\geq 2.5\sigma$ and close to which a water had been observed in the 2.4 Å native MalP structure. The final refinement statistics were $R = 0.241$, $R_f = 0.293$ (Table 1). The structure was checked with PROCHECK and showed close agreement with ideal stereochemistry as expected in view of the tight restraints used during refinement. Low RMS deviations observed for the *B*-factors of covalently linked atoms also reflect the tight restraints applied during structure refinement (Table 1). A Ramachandran plot showed 88.4% of non-glycine residues in the most favored regions, 11.4% in the additionally allowed regions, and 0.6% in the generously allowed regions. The refined protein structure had high *B*-factors (average value of 53 Å^2), but this value was consistent with that obtained from a Wilson plot (46 Å^2). The *B* values for acarbose were also high (average *B* 60 Å^2). We attempted to test if the high *B*-factors for the acarbose were correlated with occupancy. Refinements of structures in which the occupancy of acarbose was set to values of less than 1 resulted in no significant change in the *B*-factors. With occupancies below 0.75, there was residual electron density at the acarbose site in difference maps, indicating that the occupancy was probably higher than this value. Data at a higher resolution than 2.95 Å are required to determine the *B*-factors and occupancies with greater precision.

FIGURE 4: Overall view of the MalP dimer viewed approximately down the 2-fold axis of symmetry of the dimer with one subunit colored light gray and the other dark gray. Acarbose is shown binding at the catalytic site with the cyclitol sub-site furthest into the catalytic channel.

RESULTS

A summary of the X-ray data and refinement statistics for the *E. coli* MalP−acarbose complex is shown in Table 1. The electron density illustrating the binding of acarbose at the catalytic site of *E. coli* MalP is shown in Figure 3.

The catalytic site of MalP is situated in the center of the large subunit and accessible to the solvent through a 20 Å long channel. This channel forms the substrate−oligosaccharide binding site. The sub-site −1, that has been observed to bind glucose-1-P, heptulose-2-P, or glucose in the mammalian enzyme (*32*), is situated at the end of the channel, far removed from the bulk solvent and adjacent to the essential cofactor pyridoxal phosphate. In MalP, acarbose binds in sub-sites +1 to +4. These sites extend from the center of the molecule, adjacent to sub-site −1, toward the solvent (Figure 4). The two subunits of the functional dimer, labeled molecules A and B, were refined with strict NCS restraints and are therefore closely identical both for the protein and for the acarbose conformations. However, the electron density revealed some differences. Sub-site +1 is more clearly defined in subunit A, while sub-sites +2, +3,

Table 2: Geometry of Cyclitol (and Other Glucosyl Groups Bound at Site − 1) in Different α-(1,4)-Glucosyl Recognition Enzymes

enzyme complex	PDB ID no.	site[a]	torsion angles (deg)[b] ϕ_1	ϕ_2	ϕ_3	ϕ_4	ϕ_5	ϕ_6
E. coli maltodextrin phosphorylase−acarbose (this work)	2ECP	A site +1	−66	44	−10	−1	−22	54
		B site +1	−60	39	−8	−2	−19	48
pig pancreatic amylase I−acarbose (*12*)	1PPI		−68	32	8	−14	−21	61
pig pancreatic amylase II−trestatin (*13*)	1PIG		−56	34	−4	−1	−27	56
pig pancreatic amylase II−acarbose (*14*)	1OSE	site −4	−73	58	−24	3	−14	46
pig pancreatic amylase II−acarbose (*14*)	1OSE		−70	30	4	−2	−32	68
Aspergillus oryzai amylase−acarbose (*15*)	7TTAA		−72	48	−11	−7	−12	51
barley amylase−acarbose (*16*)	AMY2		−58	21	11	−1	−41	71
Bacillus subtilis (E208Q) amylase−maltopentaose (*37*)	1BAG	Glc	−63	50	−40	46	−60	68
Bacillus circulans cyclodextrin glycosyltransferase−acarbose (*17*)	2CXG		−64	45	−14	2	−20	51
Bacillus circulans cyclodextrin glycosyltransferase−maltononaose acarbose (*18*)	2DIJ		−67	55	−24	3	−14	45
Aspergillus awamori glucoamylase−acarbose (*10*)	1GAH		−63	45	−12	−5	−13	45
Aspergillus awamori glucoamylase−glucodihydroacarbose (*10*)	1GAI	DHA	−63	60	−49	44	−47	56

[a] Compound is cyclitol and binding site is sub-site −1 unless otherwise indicated. Glc, glucosyl residue; DHA, glucodihydroacarbose. [b] Torsion angles: ϕ_1 = C1C2C3C4; ϕ_2 = C2C3C4C5; ϕ_3 = C3C4C5C7(O5); ϕ_4 = C4C5C7(O5)C1; ϕ_5 = C5C7(O5)C1C2; ϕ_6 = C7(O5)C1C2C3.

and +4 are better defined in subunit B. In the MalP−acarbose complex, a glycerol molecule from the cryoprotectant (20% glycerol) occupies sub-site−1. Because the crystals were susceptible to disorder by the cryoprotectant, the soak time was limited to <5 s, but, despite this short time, cryoprotectant was able to diffuse into the crystal and bind to the catalytic site. There is no sulfate or phosphate ion at the catalytic site, in contrast to previous observations with the MalP−maltose complex (*25*). The additional dialysis steps in the present work removed any residual sulfate that had accompanied the fractional precipitation steps.

The cyclitol ring in sub-site +1 was fitted with $^2H_3$ half-chair geometry in which the torsion angle for C4−C5−C7−C1 was restrained close to zero. In Table 2 the values for the torsion angles for the cyclitol of acarbose binding to sub-site −1 in a number of different amylases, CGTases, and glucoamylases are compared. The torsion angles show some variation, as expected because of the limited resolution of the crystallographic data, but all show values close to zero for the torsion angle C4−C5−C7−C1. There appears to be no significant difference in conformation of the cyclitol ring between binding at the crucial −1 sub-site and in binding at sub-site +1, as observed in the present work, or in sub-site −4 as observed in the pancreatic amylase structure.

MalP/Acarbose Interactions. The interactions between acarbose and MalP are summarized in Figure 5. In comparison with most enzyme carbohydrate binding sites, there are rather few hydrogen bonds. The cyclitol in sub-site +1 makes hydrogen bonds from O3 to Asp339 and from O6 to Arg569. The contact from O2 to His341 (O2 to NE2 His341 = 3.5 Å) is just outside the allowed hydrogen bonding distance here taken to be 3.3 Å. The torsion angles about the amino glycosidic linkage between the cyclitol and the 6-deoxy 4-amino sugar are close to those preferred α-(1,4) linkages, and there is a characteristic intramolecular hydrogen bond between the O2 hydroxyl of the cyclitol and the O3 hydroxyl of the 6-deoxy sugar. Sub-site +2 is dominated by the carbohydrate/aromatic stacking of the glucopyranose ring with Tyr280 as noted previously in the MalP−maltose structure. The 6-deoxy sugar makes hydrogen bonds from O2 to Arg292 and from O3 to His341, as observed in the maltose structure, but there is no possibility for the hydrogen bond that is made in the maltose complex between the O6 hydroxyl and Arg569 and Lys608.

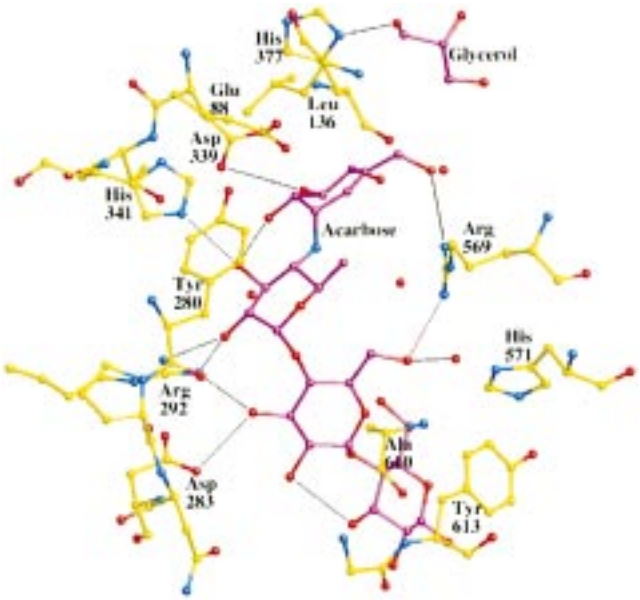

FIGURE 5: Contacts between acarbose, glycerol, and MalP. Acarbose carbon atoms are colored magenta and MalP carbon atoms yellow. The contacts of glycerol to MalP have been omitted for clarity. They include hydrogen bonds from O1 hydroxyl to N Ser674; from another hydroxyl to OG Ser674, N Gly675; ND2 Asn484; and from the third hydroxyl to ND2 Asn484 and ND1 His377.

The conformations about the glycosidic bonds of the glucosyl residues in sub-sites +2, +3, and +4 differ only slightly from the preferred conformations. There are hydrogen bonds between the O2 and O3 hydroxyls of the adjacent sugar residues, although the contact between sub-sites +2 and +3 is rather long (3.4 Å). The glucopyranose in sub-site +3 makes a number of hydrogen bonds to charged side chains of the protein. These probably provide the incentive for the small alteration in the glycosidic torsion angles between sub-sites +2 and +3. There is a long contact from O2 to Asp283 and hydrogen bonds from O3 to Arg292 and to Asp283 and from O6 to a water and to Arg 569. The glucopyranose in sub-site +4 shows a further example of carbohydrate/aromatic stacking. The sugar is stacked against Tyr613 at the entrance to the catalytic site channel. The stacking involves the A face of the sugar as does the interaction of the sugar in sub-site +2 with Tyr280. Both

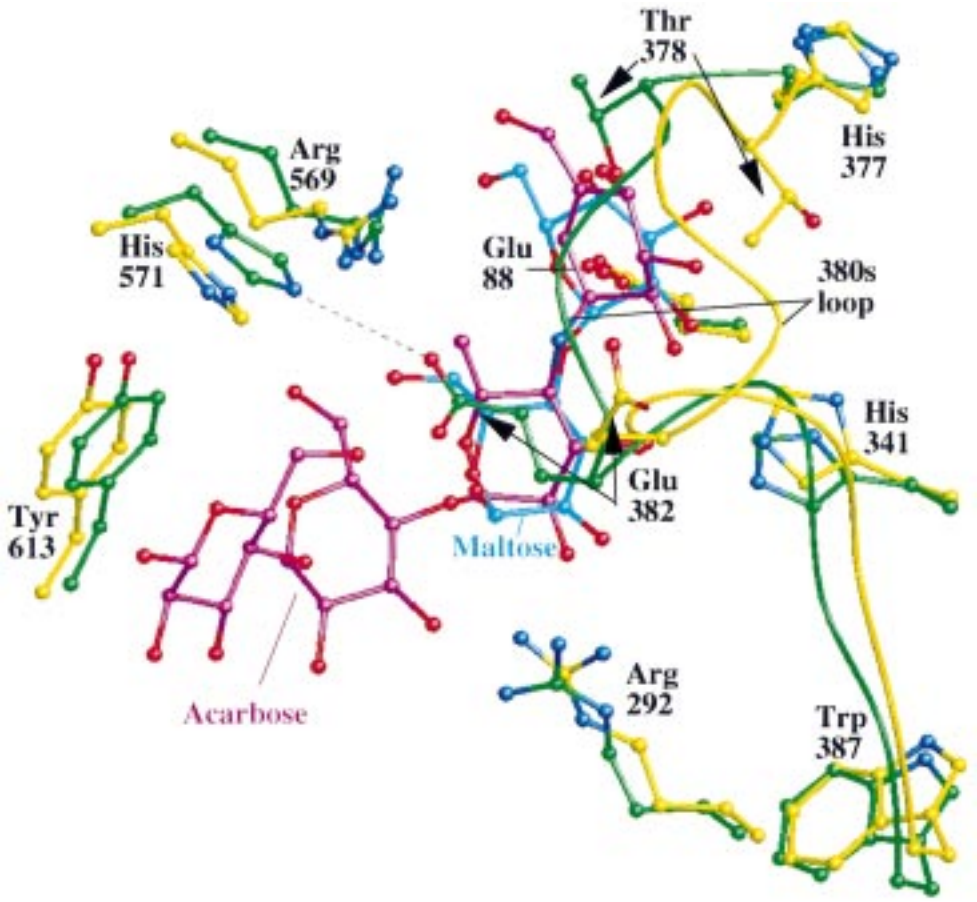

FIGURE 6: Comparison of the structures of the MalP−acarbose complex (acarbose, magenta; MalP, yellow carbon atoms) with the MalP−maltose complex (25) (maltose, cyan; MalP, green carbon atoms) showing the difference in the positions of the 380s loop and selected residues at the binding site.

Tyr280 and Tyr613 are conserved in all phosphorylases from bacteria, yeast, plants, and mammals (*33*). The carbohydrate/aromatic interactions appear a critical part of the oligosaccharide recognition site for phosphorylases.

Biochemical data have shown that maltopentaose is the minimum length oligosaccharide necessary for MalP-catalyzed phosphorolysis and maltotetraose the minimum length of primer required for MalP-catalyzed oligosaccharide synthesis with glucose 1-phosphate. The substrate specificity can be explained by the 5 sub-sites, sub-sites −1 to +4, in which sub-sites +1 to +4 are defined here by acarbose binding and sub-site −1 has been previously defined with binding studies in GP. Occupation of sub-site +4 appears important for substrate recognition. This site is close to the surface of the enzyme at the interface with the bulk solvent.

The lack of binding of acarbose in sub-site −1 may arise from several factors. First, sub-site −1 is blocked by a glycerol molecule from the cryoprotectant. Glycerol makes six hydrogen bonds at this site and appears well localized. Competition with glycerol may exclude acarbose binding at sub-site −1. In crystallographic studies with mammalian glycogen phosphorylase, glycerol, despite its poor affinity (K_i approximately 4% v/v or 540 mM), was able to compete successfully with a much higher affinity ligand for sub-site-1 (*34*). Second, occupation of sub-sites −1 and +1 simultaneously appears to require an alteration from the major minimum free energy conformation to the secondary minimum free energy conformation of the oligosaccharide (*25*). Although such a conformation is accessible to acarbose, it may require some energy. If the cyclitol of acarbose were to bind in sub-site −1, then the acarbose molecule would span sub-sites −1 to +3. This binding mode would lose the important stacking interaction of sub-site +4 with Tyr613. The $^2H_3$ half-chair conformation of the acarbose cyclitol ring is different from the $^1C_4$ chair conformation of an undistorted glucose residue and from the $^4H_3$ half-chair or sofa conformation expected for a transition state structure. However, sub-site −1 in both MalP and GP is fairly open, and modeling suggests that the $^2H_3$ cyclitol could be accommodated at sub-site −1 without bad contacts. Thus, the cyclitol is unlikely to be excluded from sub-site −1 for stereochemical reasons.

Conformational Changes. The MalP−acarbose complex more closely resembles the native MalP structure than the MalP−maltose complex (rmsd for 796 Cα atoms = 0.37 Å and 0.91 Å, respectively). In the previously determined MalP−maltose structure, there was a dramatic closure of the catalytic channel caused mostly by a shift in the 380s loop (residues His377−Trp387) so that residue Glu382 made a salt link to His571. In the MalP−acarbose complex, there is only a small shift in this loop relative to the native MalP structure so that some of the interactions made to the maltose (e.g., Glu382) are not made in the acarbose complex (Figure 6). There is a shift of about 1 Å in the position of the cyclitol ring compared to the position of the maltose glucopyranosyl in sub-site +1. The presence of the sp^2-hybridized carbon

C7 in the cyclitol ring prevents the interaction that is observed in the MalP−maltose complex between the carboxyl side chain of Glu88 and the ether oxygen O5 of glucose. The shift of the cyclitol relieves this contact and places the cyclitol closer to His341. In the MalP−acarbose structure, Thr378 is flipped away from sub-site +1 and forms a hydrogen bond with Asn376. Thr378 does not participate in a hydrogen bond to the O4 hydroxyl of the cyclitol in sub-site +1, an interaction that was observed with the MalP−maltose complex. Leu379 is twisted in its hydrophobic pocket and moves closer to Ala673. From Met 380 onward, the conformation of the 380s loop in the MalP−acarbose complex is very similar to that observed for the native MalP structure. The more open structure of the MalP−acarbose complex allows the acarviosine group to be accommodated in a different position that avoids the close contact between C7 and Glu88. Since the closure of the 380s loop is associated with the binding of the natural oligosaccharide maltose in the MalP−maltose structure and is inhibited by the presence of the unnatural cyclitol in the MalP−acarbose structure, we consider that closure of the 380s loop is likely to be a feature in substrate recognition.

DISCUSSION

The present crystallographic studies show that acarbose binds to MalP in sub-sites +1 to +4 and has allowed experimental identification of sub-sites +3 and +4 at the catalytic site of a phosphorylase for the first time. Recognition at sub-sites +2 and +4 involves carbohydrate/aromatic stacking interactions with two tyrosine residues, Tyr280 and Tyr613. These tyrosines are conserved in all phosphorylases sequenced so far (*33*). Carbohydrate/stacking interactions are a key feature of the recognition sites of a large number of carbohydrate recognition enzymes (*35*). Initially the glycogen phosphorylase catalytic site appeared to be an exception to this rule because sub-site −1, identified in numerous studies with the mammalian enzyme, involved no aromatic interactions. The present results show that carbohydrate/aromatic interactions are important in phosphorylase for direction of specificity and conformation of oligosaccharide substrate but at sub-sites removed from the immediate vicinity of catalysis.

Acarbose is a weak inhibitor of MalP at pH 6.5 [preliminary work suggests a K_i >5 mM (R. Schinzel, unpublished results)]. The present structure shows that, in addition to the contributions of the aromatic residues, there are a number of hydrogen bonds to charged residues that contribute to the binding energy. However, in contrast to high-affinity carbohydrate binding sites where each of the peripheral hydroxyl groups on a sugar is involved in at least two hydrogen bonds (*35*), the hydrogen bonds made by acarbose are relatively sparse. Some hydroxyls (e.g., the O4 hydroxyl of the cyclitol) do not participate in hydrogen bonds, and others (e.g., the O2 hydroxyl of the sugar in sub-site +3 and the O2 hydroxyl of sub-site +4) participate only in intramolecular hydrogen bonds. The sugar in sub-site +4 makes no strong hydrogen bonds to the protein and is partially exposed to the solvent.

In the MalP−acarbose complex, there are no ionic interactions with the 4-amino group that links the cyclitol to the 6-deoxy sugar. In the α-(1,4) glycosidic enzymes (amylases, glucoamylase, CGTase), the catalytic site is comprised of two carboxyl groups. One carboxyl acts as a general acid and protonates the glycosidic oxygen. The other carboxylate acts either as an electrostatic stabilizing group or a nucleophile, in those enzymes where the reaction proceeds with retention of configuration, or as a catalytic base that promotes the attack by water in those enzymes where the reaction proceeds with inversion of configuration. In each of the glucohydrolase−acarbose complexes, there is a strong interaction between the acidic carboxyl group and the amino nitrogen. In contrast to the glucohydrolases, phosphorylase does not use carboxyl residues in catalysis but employs the substrate phosphate both as the general acid and as the electrostatic stabilizing group for the reaction (*32*). However, to exploit an interaction between the amino group and the phosphate, acarbose would have to bind in sub-sites −1 to +3 and thus would lose the aromatic interaction with Tyr613 at sub-site +4. The lack of a charge interaction with the amino group and the lack of compensation of hydrogen bonding groups as the acarbose is transferred from the bulk solvent to the buried catalytic site may partly explain the low affinity of acarbose for MalP.

Acarbose is also a poor inhibitor (K_i = 26 mM) of rabbit skeletal muscle glycogen phosphorylase-a (GPa) in competition studies with 30 mM maltopentaose. The competitive inhibition suggests that acarbose may also bind to the catalytic site of GP. Crystallographic binding studies with GPa showed that acarbose bound, in its major minimum free energy conformation, at the glycogen binding site on the surface of the less active form (T state) of GPa and not at the catalytic site (*36*). In T state GPa, residues 281−285 block the catalytic site. Movement of this loop is a critical part of the activation process, and a conformational change of Tyr280 is required to provide oligosaccharide recognition. This explains why no binding of acarbose at the catalytic site was observed with GPa. MalP lacks the glycogen storage site as a consequence of sequence changes (*22*); hence, there can be no binding in this region on the outside of the molecule in MalP. However, in MalP the oligosaccharide recognition site is present at the catalytic site (*22*) to provide for acarbose binding at this site.

Acarbose binds to MalP in its major minimum free energy conformation that is characterized by intramolecular hydrogen bonds between O2 and O3 hydroxyls of adjacent sugar residues. The crystallographic results demonstrate that the catalytic site channel for sub-sites +1 to +4 can accommodate an oligosaccharide in a conformation that is close to the preferred conformation. The sites occupied and the glycosidic torsion angles are summarized in Table 3. The torsion angles ϕ [O5(C7)−C1−O4′(N4′)−C4′] and ψ (C1−O4′(N4′)−C4′−C5′) are close to the minimum free energy values for α-(1,4)-linked glucosyl residues.

Bock et al. (*8*) have shown that acarbose may adopt two different conformations in solution characterized by different torsion angles about the amino glycosidic linkage. The major conformation at alkali pH corresponds to a conformation close to the preferred conformation for α-(1,4) linked glucosyl oligosaccharides. At acid pH, a second conformation that occupies a secondary energy minima from energy diagrams (*6*) becomes populated to a significant degree (Figure 2).

Binding of acarbose and its derivatives to a number of amylases, CGTase, and glucoamylase has been reported. The

Table 3: Binding Modes and Torsion Angles for Acarbose and Related Compounds Bound to α-(1,4)-Glucosyl Enzymes

(a) Binding Modes

enzyme complex	PDB ID no.	subsites −4	−3	−2	−1	+1	+2	+3	+4
E. coli maltodextrin phosphorylase−acarbose (this work)	2ECP					C	DG	G	G
pig pancreatic amylase I−acarbose	1PPI		G	G	C	DG	G		
pig pancreatic amylase II−trestatin	1PIG		G	G	C	DG	G	G	
pig pancreatic amylase II−acarbose	1OSE	C	DG	G	C	DG	G		
Aspergillus oryzai amylase−acarbose	7TAA		G	G	C	DG	G	G	
barley amylase−acarbose	2AMY				C	DG	G		
Bacillus subtilis (E208Q) amylase−maltopentaose	1BAG		G	G	G	G	G		
Bacillus circulans cyclodextrin glycosyltransferase−acarbose	2CXG[b]			G	C	DG	G		
Bacillus circulans cyclodextrin glycosyltransferase−maltononaose inhibitor[b]	2DIJ[b]	G	G	G	C	DG	G		
Aspergillus awamori glucoamylase−acarbose	1GAH				C	DG	G	G	
Aspergillus awamori glucoamylase−glucodihydroacarbose	1GAI				DHA	DG	G	G	

(b) Torsion Angles[c]

	sites −2:−1			sites −1:+1			sites +1:+2			sites +2:+3			sites +3:+4		
PDB ID no.	ϕ	ψ	d	ϕ	ψ	d	ϕ	ψ	d	ϕ	ψ	d	ϕ	ψ	d
2ECP							124	−112	2.5	81	−123	3.4	87	−149	3.1
							124	−114	2.5	82	−123	3.5	80	−140	2.9
1PPI	90	−150	3.9	18	−149	5.4	114	−100	2.8						
1PIG	88	−146	3.8	7	−143	5.2	111	−111	2.8	108	−116	2.7			
1OSE	80	−150	4.2	18	−147	5.2	108	−110	2.9						
7TAA	120	−102	2.9	33	−152	5.3	109	−120	2.7	122	−108	2.6			
2AMY				−2	−122	5.3	90	−114	3.3						
1BAG	87	−152	3.5	29	−148	5.1	109	−125	2.7						
2CXG	110	−100	3.0	23	−146	5.0	100	−107	2.9						
2DIJ	112	−102	3.0	19	−139	5.1	106	−110	2.7						
1GAH				104	−113	3.1	91	−180	4.1	111	−117	2.8			
1GAI				100	−116	3.2	97	174	4.1	106	−112	3.0			

[a] Abbreviations: G, α-D-glucose; C, cyclitol of acarbose; DG, 4,6-dideoxy-α-D-glucose of acarbose; DHA, glucodihydroacarbose. [b] High-resolution data refinement has established the indicated mode of binding to CGTase (*19*). The maltononaose−acarbose complex has glucose residues in sites −7 to −2. [c] ϕ = torsion angle O5(C7)−C1−O4′(N4′)-C4′. ψ = torsion angle C1−O4′(N4′)−C4′−C5′. d = distance O2...O3′. Torsion angles for sub-sites −2 to +4 are given: other sites are occupied in some glucosidase complexes.

binding sites are summarized in Table 3a [following the nomenclature of Davies et al. (*24*)], and the torsion angles are given in Table 3b. The major minimum free energy conformation is characterized by (ϕ, ψ) values of (110 ± 12°, −113 ± 11°) and the secondary minimum energy conformation by (ϕ, ψ) values of (18 ± 10°, −143 ± 9°). In each of the different species of amylase studied and in the *Bacillus circulans* CGTase, acarbose binds with the cyclitol in the −1 sub-site with $^2H_3$ geometry (Table 2) and with the secondary minimum energy conformation between the cyclitol and the 6-deoxy sugar (Table 3b). This conformation is characterized by the lack of the hydrogen bond between O2 and O3′ (average distance 5.2 Å). The crystal structure of an inactive mutant (Glu208Gln) of *B. subtilis* amylase co-crystallized with maltopentaose and acarbose (*37*) indicated a pentasaccharide bound across the catalytic site (Table 3a). The density was interpreted as maltopentaose, although the less likely possibility that the density represented a modified acarbose processed by transglycosylation by the inactive mutant could not be excluded. The glucosyl residue at sub-site −1 in the assumed amylase−maltopentaose structure showed no apparent distortion from the usual chair geometry (Table 2). Thus, it appears that sub-site −1 in the amylases and other enzymes can accommodate both the half-chair geometry of the cyclitol and the chair geometry of a glucosyl residue.

In *Aspergillus awamori* glucoamylase, an *endo*-glucosidase with a reaction that proceeds with inversion of configuration, acarbose binds in its major minimum energy conformation, similar to that observed for acarbose binding to MalP (Table 3b). There is a hydrogen bond between O2 and O3′ (3.1 Å) between the cyclitol in sub-site −1 and the 6-deoxyglucose in sub-site +1. The observation that acarbose can act as an inhibitor of a number of different glucosidases appears in part to be due to the ability of acarbose to adopt two different conformations around the amino glycosidic bond between the cyclitol and the 6-deoxy sugar. It is striking that the affinity of glucoamylase for acarbose ($K_i = 10^{-10}$ M) is very much greater than that of the amylases ($K_i = 10^{-6}$). Glucoamylase binds acarbose in its preferred minimum energy conformation, and the amylases bind acarbose in the secondary minimum energy conformation. Estimates of the energy difference between the two conformations vary in the range of 2−4.5 kcal mol^{-1} (*8*, *38*), corresponding to a difference in K_i of between 30- and 1800-fold, if the binding energy is used to promote the higher energy conformation. It is possible that the lower affinity of acarbose for amylase reflects, in part, the conformational energy cost to bring acarbose from its major minimum free energy conformation to its secondary minimum free energy conformation. The low affinity of acarbose for MalP, where acarbose adopts the major minimum free energy conformation, is due to other reasons. These include few hydrogen bonds made in the complex, the lack of a charge interaction with the amino linking group between the cyclitol and the 6-deoxy sugar, and the restriction of the conformational change that closes the catalytic site by the cyclitol.

ACKNOWLEDGMENT

Acarbose (BAYG5421) was kindly provided by H. Bischoff at Bayer AG, Wuppertal. We are grateful to the support staff at the Elettra Synchrotron for their help with the use of the beam line. We also thank Dr. R. Schinzel and Professor D. Palm, who provided us with partially purified MalP, Claire McCleverty and Eilis Byrne for help with expression and purification of *E. coli* maltodextrin phosphorylase, M. E. M. Noble for his program OGLOBJECTS, and R. Bryan for help with computing. We are grateful to all authors who sent coordinates prior to availability in the PDB.

REFERENCES

1. Truscheit, E., Frommer, W., Junge, B., Muller, L., Schmidt, D. D., and Wingender, W. (1981) *Angew. Chem., Int. Ed. Engl. 20*, 744−761.
2. Bischof, H. (1995) *Clin. Invest. Med. 18*, 303−311.
3. Scheen, A. J. (1997) *Drugs 54*, 355−368.
4. Quigley, G. J., Sarko, A., and Marchessault, R. H. (1970) *J. Am. Chem. Soc. 92*, 5834−5839.
5. Rees, D. A., and Smith, P. J. C. (1975) *J. Chem. Soc., Perkin Trans. 2*, 836−840.
6. Dowd, M. K., Zeng, J., French, A. D., and Reilly, P. J. (1992) *Carbohydr. Res. 230*, 223−244.
7. Bock, K., and Pedersen, H. (1984) *Carbohydr. Res. 132*, 142−149.
8. Bock, K., Meldal, M., and Refn, S. (1991) *Carbohydr. Res. 221*, 1−16.
9. Aleshin, A. E., Firsov, L. M., and Honzatko, R. B. (1994) *J. Biol. Chem. 269*, 15631−15639.
10. Aleshin, A. E., Stoffer, B., Firsov, L. M., Svensson, B., and Honzatko, R. B. (1996) *Biochemistry 35*, 8319−8328.
11. Stoffer, B., Aleshin, A. E., Firsov, L. M., Svensson, B., and Honzatko, R. B. (1995) *FEBS Lett. 358*, 57−61.
12. Qian, M., Haser, R., Buisson, G., Duée, E., and Payan, F. (1994) *Biochemistry 33*, 6284−6294.
13. Machius, M., Vértesy, L., Huber, R., and Wiegand, G. (1996) *J. Mol. Biol. 260*, 409−421.
14. Gilles, C., Astier, J.-P., Marchis-Mouren, G., Cambillau, C., and Payan, F. (1996) *Eur. J. Biochem. 238*, 561−569.
15. Brzozowski, A. M., and Davies, G. J. (1997) *Biochemistry 36*, 10837−10845.
16. Kadziola, A., Søgard, M., Svensson, B., and Haser, R. (1998) *J. Mol. Biol. 278*, 205−217.
17. Strokopytov, B., Penninga, D., Rozeboom, H. J., Kalk, K. H., Dijkhuizen, L., and Dijkstra, B. W. (1995) *Biochemistry 34*, 2234−2240.
18. Strokopytov, B., Knegtel, R. M. A., Penninga, D., Rozeboom, H. J., Kalk, K. H., Dijkhuizen, L., and Dijkstra, B. W. (1996) *Biochemistry 35*, 4241−4249.
19. Mosi, R., Sham, H., Uitdehaag, J. C. M., Ruiterkamp, R., Dijkstra, B. W., and Withers, S. G. (1998) *Biochemistry 37*, 17192−17198.
20. Ford, L. O., Johnson, L. N., Machin, P. A., Phillips, D. C., and Tijian, R. (1974) *J. Mol. Biol. 88*, 349−371.
21. Raibaud, O., and Schwartz, M. (1984) *Annu. Rev. Genet. 18*, 207−231.
22. Watson, K. A., Schinzel, R., Palm, D., and Johnson, L. N. (1997) *EMBO J. 16*, 1−14.
23. Becker, S., Palm, D., and Schinzel, R. (1994) *J. Biol. Chem. 269*, 2485−2490.
24. Davies, G. J., Wilson, K. S., and Henrissat, B. (1995) *Biochem. J. 321*, 557−559.
25. O'Reilly, M., Watson, K. A., Schinzel, R., Palm, D., and Johnson, L. N. (1997) *Nat. Struct. Biol. 4*, 405−412.
26. Schinzel, R., and Palm, D. (1990) *Biochemistry 29*, 9956−9962.
27. Schinzel, R., Palm, D., and Schnackerz, K. D. (1992) *Biochemistry 31*, 4128−4133.
28. CCP4 (1994) *Acta Crystallogr., Sect. D D50*, 760−763.
29. Navaza, J. (1990) *Acta Crystallogr. A50*, 157−163.
30. Brünger, A. T. (1992) *X-PLOR: Version 3.1; a system for protein crystallography and NMR*, Yale University Press, New Haven.
31. Murshudov, G. N., Vagen, A. A., and Dodson, E. J. (1997) *Acta Crystallogr. D53*, 240−255.
32. Johnson, L. N., Acharya, K. R., Jordan, M. D., and McLaughlin, P. J. (1990) *J. Mol. Biol. 211*, 645−661.
33. Newgard, C. B., Hwang, P. K., and Fletterick, R. J. (1989) *CRC Crit. Rev. Biochem. Mol. Biol. 24*, 69−99.
34. Gregoriou, M., Noble, M. E. M., Watson, K. A., Garman, E. F., Krulle, T. M., de la Fuenta, C., Fleet, G. W. J., Oikonomakos, N. G., and Johnson, L. N. (1998) *Protein Sci. 7*, 915−927.
35. Quiocho, F. A. (1986) *Annu. Rev. Biochem. 55*, 287−315.
36. Goldsmith, E. J., Fletterick, R. J., and Withers, S. G. (1987) *J. Biol. Chem. 262*, 1449−1455.
37. Fujimoto, Z., Takase, K., Doui, N., Momma, M., Matsumoto, T., and Mizuno, H. (1998) *J. Mol. Biol. 277*, 393−407.
38. Coutinho, P. M., Dowd, M. K., and Reilly, P. J. (1997) *Proteins: Struct. Funct., Genet. 27*, 235−248.

BI9828573